

Modifications of Hydrophobic Value and Hydrophobic Moment Value of Cationic Model Peptides for Conversion of Peptide–Membrane Interactions

Junichi Taira,[1] Sachi Furukawa,[2] Tomomitsu Hatakeyama,[2] Haruhiko Aoyagi,[2,†] and Hiroaki Kodama*[1]

[1]Department of Chemistry, Faculty of Science and Engineering, Saga University, Saga 840-8502

[2]Department of Applied Chemistry, Faculty of Engineering, Nagasaki University, Nagasaki 852-8521

Received November 2, 2007; E-mail: hiroaki@cc.saga-u.ac.jp

The hydrophobic value $\langle H \rangle$ and hydrophobic moment value $\langle \mu \rangle$ of helical peptides correlate with membrane–peptide interactions such as ion channel forming or membrane perturbation. In this paper, two cationic amphiphilic peptides, ALSAALKAALSWASLAAKLAASLA-amide (Ap) and KK-ALSAALKAALSWASLAAKLAASLA-KK-amide (KAp), consisting of 24 and 28 amino acid residues, respectively, were synthesized to acquire antimicrobial activities and to reduce the high hemolytic activity of cationic helical peptide, LARLLARLLARLLRALLRALLRAL-amide (4_6), reported previously. Both peptides were designed to possess higher hydrophobic values and lower hydrophobic moment values than those of 4_6. Circular dichroism (CD) measurements of the peptides showed that the peptides had lower α-helical content than that of 4_6 in aqueous solutions as well as the membrane mimetic environments. 4_6 did not show any antibacterial activity whereas KAp and Ap had antibacterial activities against Gram-positive and -negative bacteria. In contrast, the hemolytic activities of Ap and KAp decreased to less than that of 4_6. Electrophysiological experiments were carried out to compare ion channel formation. Both peptides showed ion conductance patterns distinguishable from the patterns of 4_6 and pore forming with flexible structures was suggested. In addition, the flanking cationic residues of KAp tended to increase the channel opening durations.

Amphiphilic cationic peptides are a class of antibacterial peptides some of which form ion channels by self-aggregation in cellular membranes.[1–3] Structure activity relationship studies of ion channel forming by cationic peptides have been developed, however, the relationships between the ion channel properties and antibacterial or hemolytic activities are still a matter of debate.[4] We previously reported that an amphiphilic α-helical peptide, 4_6 (Figure 1a), which was long enough to span the lipid bilayer, could form a cation-selective ion channel in the diphitanoyl phosphatidylcholine (DPhPC) bilayer.[5–7] However, in spite of the ion channel forming ability, 4_6 was disqualified as a candidate antibacterial agent due to its negligible or absent antibacterial activity and strong hemolytic activities.[5,7] Enhancement of the antibacterial activity and decrease in hemolytic activity have been considered as primary tasks for therapeutic application. To overcome these issues, modifications of the hydrophobic values $\langle H \rangle$ and hydrophobic moment values $\langle \mu \rangle$, which correlate with the antibacterial activity and/or hemolytic activity, are promising approaches.[8] Furthermore, to clarify the ion channel properties associated with the biological activities would be useful for an ion channel mediated antibacterial peptide design. To assess the ion channel activity of a peptide with antibacterial (or hemolytic) activities would help distinguish whether these biological activities are mediated via the ion channel forming process. In this study, two cationic peptides, Ap and KAp, modified analogs based on 4_6, were designed as better model peptides for an antibacterial and ion channel peptide design (Figure 1a). The structures and behaviors against lipid membranes, biological activities and ion channel properties of Ap and KAp were examined.

Results and Discussion

Peptide Design and Synthesis. Since 4_6 contains many Leu residues as hydrophobic components and Arg residues as hydrophilic ones on opposite sides of the helical wheel, this peptide has a large hydrophobic moment value of 0.482, and the strong membrane perturbation was attributable to that value.[9] To provide a lower hydrophobic moment value, Leu and Ala in 4_6 were reversed and the Arg residues were substituted with Lys or Ser residues. The hydrophobic moment values of KAp and Ap were 0.207, and flanking the four Lys residues of KAp was not considered for determining the values. Increasing the total positive charge often, but not necessarily, results in enhanced antibacterial activities because the cationic features of an antibacterial peptide allow them to interact more effectively with the negatively charged lipopolysaccharide (LPS) and/or cytoplasmic bacterial cellular membranes.[10] The net charges of KAp, Ap, and 4_6 are +7, +3, and +7, respectively. The K–K sequences were attached at the N- and C-terminal flanking portions of KAp to increase the total positive charge without alteration of the hydrophobic moment value as well as enhancement of the ion channel forming in the

† Present address: Kyushu Nutrition Welfare University, Kokurakita-ku, Kitakyushu 803-8511

Published on the web June 11, 2008; doi:10.1246/bcsj.81.733

a

KAp H-KK-ALSA-ALKA-ALSW-ASLA-AKLA-ASLA-KK-NH_2

Ap H-ALSA-ALKA-ALSW-ASLA-AKLA-ASLA-NH_2

4_6 H-LARL-LARL-LARL-LRAL-LRAL-LRAL-NH_2

b

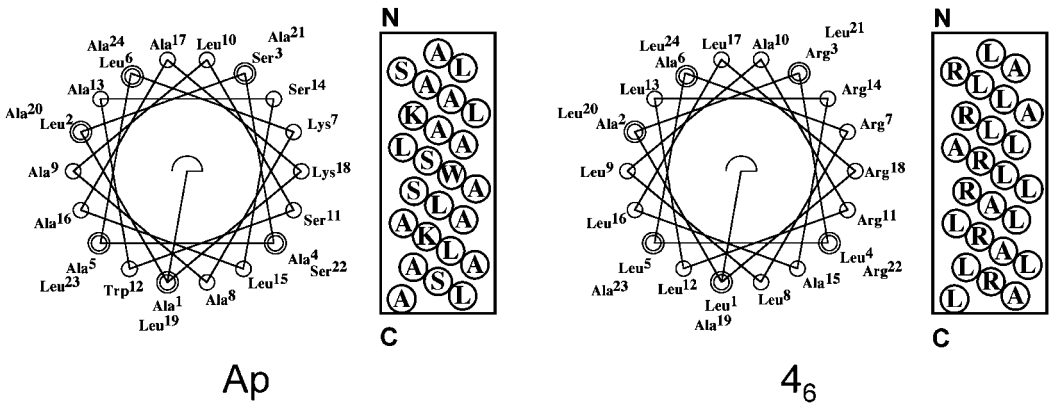

Figure 1. (a) Structures of synthetic peptides. (b) Comparison of helical wheels and helical nets of Ap and 4_6.

lipid bilayer. Davis et al. designed peptides to maintain the transbilayer orientation by attaching charged amino acid residues to each end of the peptides and performed a perpendicular peptide insertion against the lipid bilayer.[11] A Trp residue was introduced into each peptide to examine the behavior of the peptides against or in the lipid membranes by spectrophotometry. As a consequence of these substitutions, the hydrophobic values of 0.128, −0.06, and −0.123 were determined for Ap, KAp, and 4_6, respectively.[9] The peptides were synthesized by a fluorenylmethoxycarbonyl (Fmoc) solid phase peptide synthesis strategy on 4-(α-amino-2,4-dimethoxybenzyl)phenoxy (Rink amide) resin. The obtained crude products were purified by RP-HPLC. Identification of the purified peptides was done by MALDI-TOFMS and amino acid analysis, and the results were satisfactory (see Experimental Section).

CD Measurement. To explore the peptide structures in various environments, circular dichroism (CD) measurements were performed in Tris HCl buffer (pH 7.4), the buffer in the presence of egg PC or egg PC/egg PG (3:1) vesicles and the buffer in the presence of dioleoylphosphatidylcholine (DOPC) or DOPC/dioleoylphosphatidylglycerol (DOPG) (3:1) vesicles. All the peptides produced α-helix patterns, and the α-helix contents were estimated from the degree of negative minima around 222 nm (Table 1). In the buffer solution, Ap and KAp showed low helix contents. The helix contents were increased 70–80% in the presence of the egg PC or egg PC/egg PG (3:1) vesicles, however, in the presence of the DOPC or DOPC/DOPG (3:1) vesicles, they exhibited low helix contents. Generally, acyl groups of phospholipids correlate to phase-transition temperatures and fluidities of phospholipid membranes. Peptide–membrane interactions partially depend on the membrane fluidities, thus, observed helix contents of the model peptides should be influenced by the structural differences of the phospholipid components. In addition, KAp showed higher helical contents in the presence of acidic PC/PG membranes than those in the presence of zwitterionic PC membranes. Extended cationic features of KAp could allow electrostatically peptide interactions to the acidic membranes. 4_6 showed high α-helix contents under various conditions, and the rigid helical structure was concerned. Modifications of the 4_6 caused a helix disorder in aqueous solutions and helix forming in specific membranes.

Table 1. Helical Contents of Synthetic Peptides in Various Environments

Peptides	α-Helical content/%[a]				
	Buffer (pH 7.4)	Egg PC	Egg PC/ Egg PG (3/1)	DOPC	DOPC/ DOPG (3/1)
KAp	24	56	74	7	16
Ap	23	85	80	34	42
4_6	52	87	75	100	99

a) Helix contents were calculated according to the method of Scholtz et al.[19]

Table 2. Antimicrobial Activity of the Synthetic Peptides

Peptides	MICs/μg mL^{-1}			
	S. aureus NBRC 12732	*B. subtilis* NBRC 3134	*E. coli* NBRC 12734	*P. aeruginosa* NBRC 12582
KAp	2	2	8	4
Ap	32	8	64	>64
4_6	>64	>64	>64	>64

Antibacterial and Hemolytic Activities. The antibacterial activity was examined by serial solution dilution methods using two Gram-positive bacteria (*S. aureus* and *B. subtilis*) and two Gram-negative bacteria (*E. coli* and *S. aureginosa*). The minimum inhibitory concentrations (MICs) of the peptides are listed in Table 2. As was reported, 4_6 showed no antibacterial activity against any of the bacteria and it is likely that the

long and rigid structure of 4_6 is also unfavorable for passing through the non-lipid layer of bacterial cell membranes.[6,7] However, the antibacterial activities of Ap and KAp were moderated. It was suggested that the optimized peptide structures allowed smooth interactions against the bacterial cell membranes. It is noteworthy that KAp showed high antibacterial activity against even Gram-negative bacteria. Since peptides with many cationic amino acid residues were found to be active against Gram-negative bacteria, the present result is consistent with previous findings.[10,12]

The hemolytic activity was assayed using fresh rabbit blood cells (Figure 2). Although 4_6 showed 100% activity at a peptide concentration of 10 μM (1 M = 1 mol dm^{-3}), Ap and KAp had 100% activities at peptide concentrations of 30 and 100 μM, respectively. In spite of the low hydrophobicity, 4_6 had very strong hemolytic activity. Since it has been believed that the strong hemolytic activity was attributable to the high hydrophobic moment value, lower hydrophobic moment values of KAp and Ap may decrease hemolytic activities.[8] A remarkable lowering of the hemolytic activity indicates that Ap and KAp more mildly interact with blood cell membranes than 4_6 thus it seems that they would be useful as antibacterial agents. The higher hemolytic activity of Ap than KAp may be due to the higher hydrophobicity of the former than the latter. This result is reasonable, because the outer membrane of a red blood cell scarcely contains any anionic phospholipids, and consequently, the driving force of interaction of the peptides with the phospholipid membrane is a hydrophobic interaction.

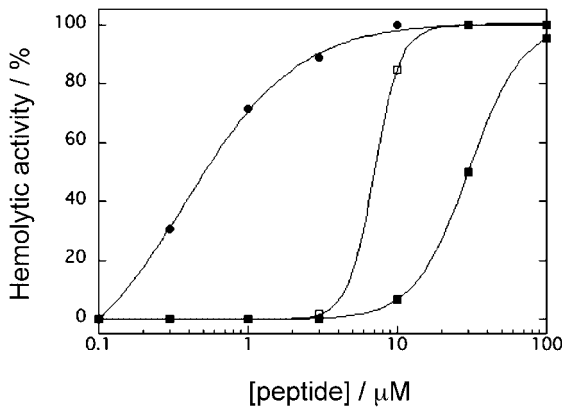

Figure 2. Hemolytic activity of synthetic peptides. To a rabbit erythrocyte solution was added a TSB solution followed by the peptides. The supernatant was diluted fivefold with TSB solution and monitored at 413 nm. To measure the absorbance for 100% activity, 10% Triton X-100 instead of the peptide was added to the erythrocyte solution. EC_{50} of 4_6 (●), KAp (■), and Ap (□) are 0.5, 30.2, and 7.1 μM, respectively.

Tryptophan Fluorescence and Calcein Leakage. The tryptophan fluorescence and calcein leakage activity of the peptides were measured to confirm that the peptides could interact with the phospholipid bilayer mimicking the bacterial cell membrane. The results of the tryptophan fluorescence measurements are shown in Figure 3a. In aqueous solution, the wavelength maxima of the peptides were 348–352 nm, indicating that the Trp residues were in a hydrophilic environment. With increasing concentration of the egg PC/egg PG (3:1) phospholipid vesicles, the fluorescent maximum shifted to a shorter wavelength. The fluorescent maxima were 315–320 nm at a [lipid]/[peptide] ratio of 75:1. This result indicates that the Trp residues in the peptides were embedded in the membrane, because the blue shift of the maximum wavelength and increase in the fluorescence intensity mean the movement of the Trp residue into a more hydrophobic region of the membrane. The calcein leakage activity of the peptides was examined using calcein-entrapped egg PC/egg PG (3:1) vesicles (Figure 3b). Ap and KAp showed similar leakage activities. Based on these results, it was expected that both peptides have a potent peptide–membrane interaction and membrane perturbation against bacterial cell membranes.

Outer and Inner Membrane Permeability. The outer membranes of Gram-negative bacteria contain a LPS as the main component,[13] which plays an important role in membrane translocation. Bacteria are often resistant to antibiotics by using the LPS as a defense wall. *N*-Phenyl-1-naphthylamine (NPN), a hydrophobic fluorescent probe, cannot penetrate

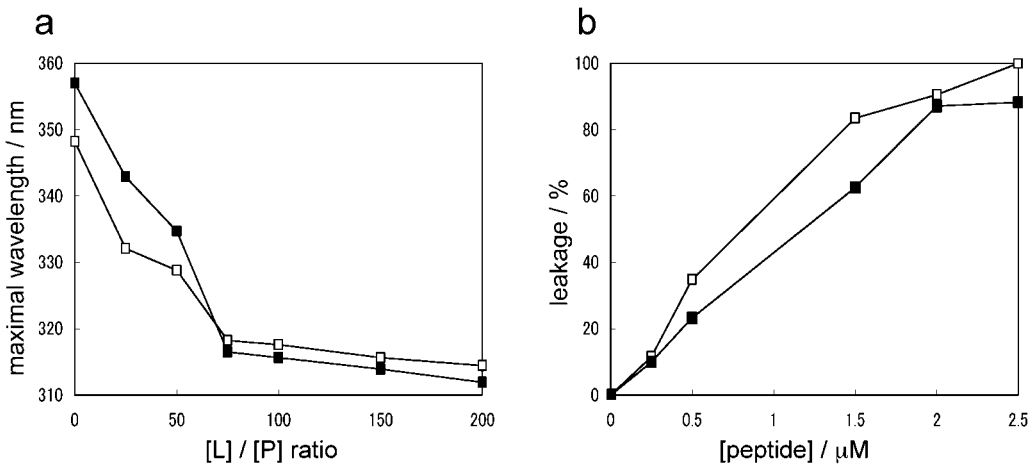

Figure 3. (a) Trp titration measurement. The peptide concentration was 10 μM and the ratio of lipid to peptide was changed from 0 to 200. The samples were excited at 280 nm. (b) Calcein leakage measurements of the peptides for egg PC/egg PG (3:1) SUVs. [Lipid] = 70 μM, 25 °C, λ_{ex} = 495 nm and λ_{em} = 515 nm. Leakage was measured 2 min after doping of the peptides. The 100% calcein release was determined by the addition of 10% Triton X-100. KAp (■) and Ap (□).

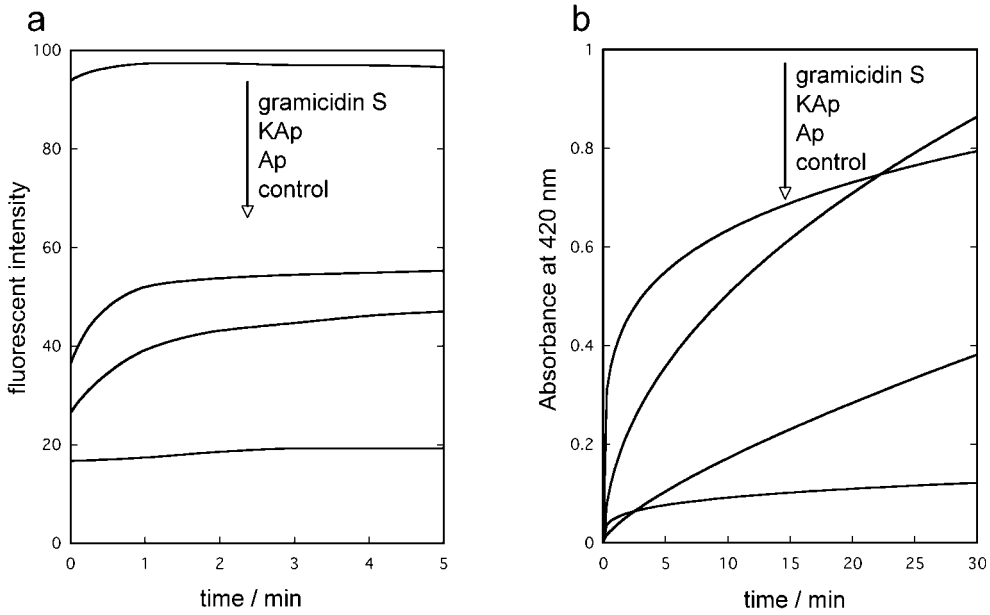

Figure 4. (a) Outer membrane permeabilization activities of the peptides assesed by the NPN uptake in *E. coli*. [peptide] = 32 μM, [NPN] = 5 μM, λ_{ex} = 350 nm, and λ_{em} = 420 nm. (b) Inner membrane permeabilities of peptides assesed by the ONPG uptake in *E. coli*. [peptide] = 32 μM and [ONPG] = 5 μM.

through the intact bacterial outer membrane, but it is taken up into the membrane interior when the membrane is disturbed.[14] Since the fluorescence intensity of NPN increases in a hydrophobic environment, it is quite applicable to the permeability measurement. The outer membrane permeability of the peptides is shown in Figure 4a. Although KAp had a higher permeability than Ap, the difference between the permeabilities of the peptides was small. The fluorescence intensity first rapidly increased and then slowly, suggesting that a structural change in the outer membrane rapidly occurred.

The inner membrane permeability was evaluated by measuring β-galactosidase activity using *o*-nitrophenyl β-galactopyranoside (ONPG) as a substrate.[15] When the permeability of the inner membrane is increased by the peptide, ONPG moves into the cytoplasm, and is hydrolyzed by β-galactosidase to produce *o*-nitrophenol, which is colored under weakly alkaline conditions. This result is shown in Figure 4b. The absorbance at 420 nm gradually increased with the passage of time, and the order of permeability was KAp > Ap. The difference in the inner membrane permeabilities between KAp and Ap was clear. The interaction and accumulation of KAp against the acidic bacterial cellular membrane would be facilitated by the extended cationic features of the peptide. It is almost certain that the antibacterial activities of KAp and Ap are due to peptide-mediated membrane perturbation. Nevertheless, exact reasons of these high membrane permeabilities have not been clarified in the present stages. Peptide flexibility is considered as one of the possible reasons for the permeabilities.[16] The membrane translocation of the peptides and successive bacterial cell death could be attributed to the structural flexibility of the peptides.

Ion Channel Activities. Single channel measurements of KAp and Ap were carried out on the DPhPC bilayer and compared to the ion channel activities of 4_6. Figure 5 illustrates the typical ion conductance patterns of KAp and Ap and their histogram analyses. The current transitions in the patterns reflect ion permeation across the bilayer and the transition degrees correspond to the ion conductance values.[17] KAp and Ap did not perturb and destroy membranes during the measurements, however, erratic conductance patterns were significantly observed. Various conductance values were identified in the patterns of both peptides; KAp and Ap exhibited 25–80 and 20–195 pS conductance values, respectively. The observed conductance values and calculated number of helices involved in the pore formation are summarized in Table 3. Generally, the multi-level ion conduct states are caused by an increase or decrease of helix monomers involved in the ion conduct bundle formation. We concluded that the channels formed by 4_6 also contain several types of bundles with different numbers of monomers,[5] however, the calculated pore diameters of KAp and Ap correspond to only tri- or tetrameric helices.[18] The CD spectra of these two peptides recorded in the presence of DOPC media possess considerably lower helix contents than that of 4_6. Thus, it is considered that when the ion channel bundles were assembled by Ap and KAp, the bundles may have flexible structures in the zwitterionic phospholipid bilayers. In addition, KAp tends to show a longer channel opening duration than that of Ap; the contribution of the flanking Lys residues of KAp for pore stabilization was considered. Several reports performed embedding of Lys residues at each end of helices for perpendicularly helix insertion and stabilization in bilayer.[11] The termini Lys residues could be exposed in water phase on both sides of the bilayer and allow perpendicular orientation of helices against the bilayer. On the basis of these reports, the elongated channel opening duration of KAp might be caused by the facilitated perpendicular orientation of helices.

Conclusion

Numerous cationic amphiphilic peptides have been designed to clarify the relationships between their structure and

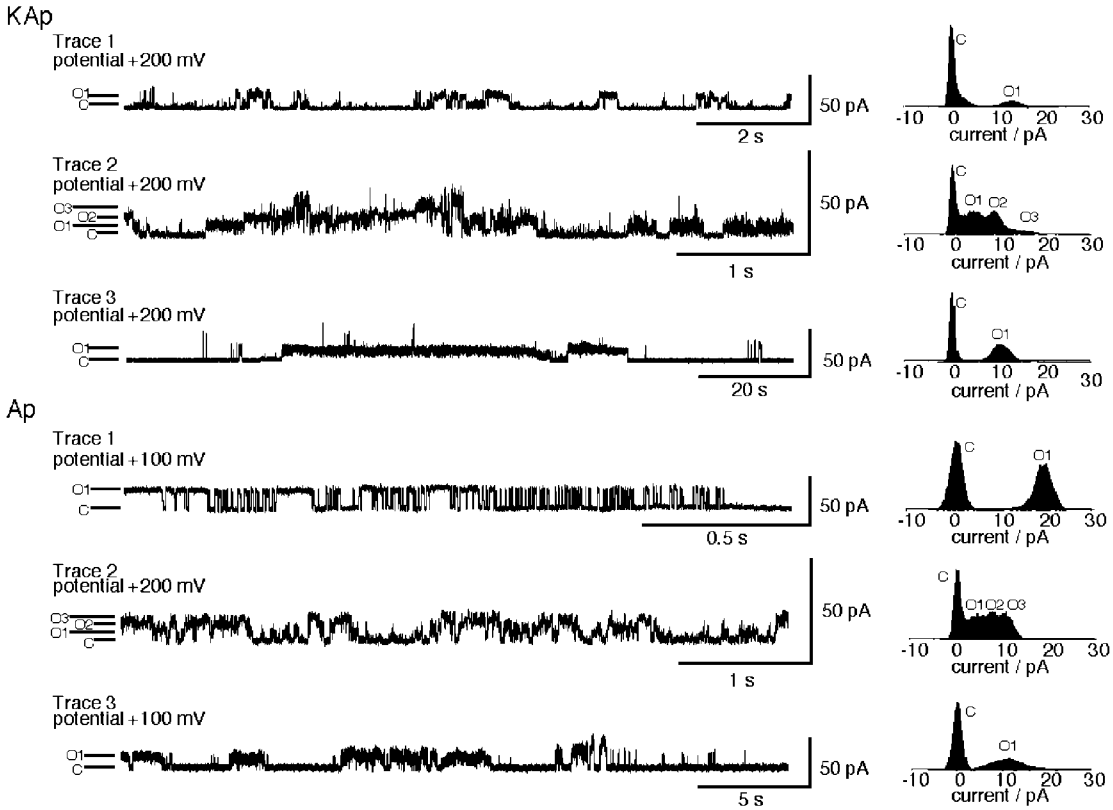

Figure 5. Ion conductance patterns of model peptides under various electrical potentials and histogram analyses. The experiment was carried out by the pipette dipping patch clamp technique at $25 \pm 2\,^{\circ}C$ and data was filtered at 1 or 2 kHz frequency. The pipettes were filled with a 0.5 M KCl solution buffered with 5 mM HEPES (pH 7.4) containing 100 nM peptides. Symbols C and $O_{1,2,3}$ denote the zero current level and open levels of channels, respectively.

Table 3. Summarized Parameters Obtained from Ion Channel Activity Measurements

Peptides	Trace number[a)]	Potentials /mV	Open state	Current /pA	Conductance values (G) /pS[b)]	Pore radius (r) /nm[c)]	Number of helices (N)[c)]
KAp	1	+200	1	13.0	65	0.12	3
	2	+200	1	5.0	25	0.07	3
			2	8.9	45	0.10	3
			3	16.0	80	0.13	3
	3	+200	1	10.7	54	0.10	3
Ap	1	+100	1	19.5	195	0.20	4
	2	+200	1	4.0	20	0.06	3
			2	7.5	38	0.09	3
			3	10.0	50	0.10	3
	3	+100	1	10.8	108	0.15	3

a) The trace numbers and open state numbers are corresponding to Figure 5. b) The conductance values (G) were calculated as $G = I/E$. c) The pore radius (r) and number of pore-forming helices (N) were estimated according to eqs 2a and 2b, respectively. The helix length (l) is 36 Å, the radius of the helix is 5.0 Å, and the bulk solution resistivity (ρ) of 500 mM KCl is 0.17 Ωm.[23]

antimicrobial activity. Much attention has been concentrated on finding peptides with strong antibacterial activity, but with no hemolytic activity for therapeutic use. In this study, we attempted to improve the antibacterial activity and lower the hemolytic activity by modification of the hydrophobic moment values and hydrophobic values of the peptides. Trp titration, dye leakage measurement and membrane permeability experiments strongly supported the interactions of model peptides against bacterial cell membranes. KAp and Ap had lower α-helix contents than that of 4_6 under several conditions due to their lower amphiphilic character. These results suggested that a high amphiphilic character is not necessary for antibacterial activity, while the activities may require peptide flexibility. In our previous study, peptide 4_6 performed ion channel activities with clearly open–close transitions. On the other hand, KAp and Ap showed erratic patterns with lower ion conductance

values. The observed biological activities were attributed to peptide-mediated membrane perturbations, ion channel activity is not a major antibacterial pathway although observed erratic ion conduction might have occurred by peptide flexibility and a stable ion channel requires a rigid helix structure.

Experimental

General. HPLC was performed on a system comprised of an 807-IT integrator (JASCO, Tokyo), two pumps PU-980 (JASCO), a UV-970 detector (JASCO), and a Rheodyne 7125 injector (Rheodyne Inc., CA, USA). A Branson bath-type sonocator (Branson, CT, USA) and Taitec Ultrasonic Processor VT-5 T (TAITEC, Saitama) were used for preparation of phospholipid vesicles. CD spectra were recorded on a JASCO J-720 spectropolarimeter (JASCO). UV and visible spectra were recorded on a Hitachi V-2000 spectrophotometer (Hitachi, Tokyo). Fluorescence spectra were recorded on a Hitachi F-3010 spectrofluorometer (Hitachi). A pipette puller (Narishige, Tokyo) was used to prepare patch clamp pipettes. Single-channel currents were amplified using an Axopatch 1D patch-clamp amplifier (Axon Instruments, Inc., CA, USA) controlled by pClamp 6 software.

H-KK-ALSAALKAALSWASLAAKLAASLA-KK-NH_2 (KAp). The peptide was synthesized by a solid-phase method using Fmoc amino acids and Rink amide resin. Coupling reagents were *N*,*N*,*N*′,*N*′-tetramethyl-*O*-(1*H*-benzotriazol-1-yl)uranium hexafluorophosphate (HBTU) and *N*-hydroxybenzotriazole (HOBt), and removal of Fmoc groups was done with 30% piperidine/DMF. Final deblocking and removing the peptide from the resin was done with trifluoroacetic acid (TFA) in the presence of *m*-cresol, ethanedithiol, and thioanisole. The cleavage cocktail was concentrated and crude product was obtained from ether precipitation. The product was purified by gel chromatography on a Sephadex G-10 column, followed by RP-HPLC on a YMC-Pack ODS column (100% H_2O–0.1% TFA and 100% acetonitrile–0.08% TFA). The structure of desired product was confirmed by MALDI-TOFMS and amino acid analysis, and peptide purity was found to exceed 95% by analytical RP-HPLC. Final yield: 6.7 mg (4.8%). MALDI-TOFMS calcd for $C_{128}H_{227}N_{36}O_{32}$ $[M + H]^+$ 2780.7, found 2782.1.

H-ALSAALKAALSWASLAAKLAASLA-NH_2 (Ap). The peptide synthesis, purification and confirmations of homogeneity were carried out by the same methods as described above. Final yield: 5.3 mg (5.3%). MALDI-TOFMS calcd for $C_{104}H_{179}N_{28}O_{28}$ $[M + H]^+$ 2268.3, found 2270.2.

Preparation of Phospholipid Vesicles. Small unilamellar vesicles of egg PC and egg PC/egg PG (3:1) were prepared for the CD measurement. Phospholipid (5 μmol) was dissolved in $CHCl_3$/MeOH (2:1 v/v, 2 mL), then dried under a stream of N_2 gas. The dried lipid was hydrated in 20 mM Tris HCl buffer (pH 7.4, 5 mL) using a bath-type sonicator. The suspension was sonicated for 10 min at 50 °C. The vesicles were allowed to stand for 30 min before the measurements were made. The lipid concentration was 1 mM.

CD Measurement. CD spectra were recorded on a CD spectropolarimeter with a thermostatted cell holder using a quartz cell of 1.0 mm path length. The peptides were dissolved in 20 mM Tris HCl buffer (pH 7.4) and a buffer containing 1 mM phospholipid vesicles. The concentration of the peptides was 20 μM. Measurements were done at 25 °C. Spectra were corrected in the range of 190–260 nm. The mean residue ellipticity is given as deg cm^2 $dmol^{-1}$, and the helix contents were calculated according to the method of Scholtz et al.[19]

Antibacterial and Hemolytic Activities. The minimal inhibitory concentration (MIC) was determined by serial solution dilution.[20] A cell suspension was diluted with tryptic soy broth (TSB) medium to 10^4 cells mL^{-1}. Various concentrations of the peptide solution were placed in test tubes, made up to 20 μL with medium, and the cell suspension (180 μL) was added. After incubation for 20 h at 37 °C, the absorbance at 620 nm was measured. Hemolytic activity was determined by the procedure of Yoshida et al.[20] Fresh rabbit blood (1 mL) was centrifuged at 2500 rpm for 3 min and the precipitates were collected. Washing with TSB solution (pH 7.4) was repeated three times. The precipitates were suspended with four-fold volumes of TSB. To rabbit erythrocyte suspension (5 μL) was added TSB solution (1 mL) followed by the peptides. The resulting suspension was incubated for 30 min at 37 °C and then centrifuged. The supernatant was diluted five-fold with TSB solution and absorbance was monitored at 413 nm. To measure the absorbance for 100% activity, 10% Triton X-100 (10 mL) instead of peptide was added to the erythrocyte suspension.

Tryptophan Titration and Calcein Leakage. The fluorescence values of Trp in the peptides were measured in Tris HCl buffer (pH 7.4) and in vesicle dispersion.[21] The peptide concentration was 10 μM and the ratio of lipid to peptide was changed from 0 to 200. The samples were excited at 280 nm and emission spectra were recorded from 310 to 360 nm wavelength. Fluorescence emission was expressed in arbitrary units. The calcein leakage experiment was performed by the procedure of Lee et al.[21] To Tris HCl buffer (pH 7.4, 2 mL) in a cuvette was added 20 μL of vesicles containing 0.1 M calcein to give a solution with a phospholipid concentration of 70 μM. To the cuvette in a holder (25 °C) was added 20 μL of an appropriate dilution of the peptides in buffer. The fluorescence intensities of calcein were monitored at 515 nm (excited at 495 nm) and measured 2 min after adding the peptides. Calcein leakage was determined as follows. To measure the fluorescence intensity for 100% calcein release, 10% Triton X-100 (10 μL) was added to dissolve the vesicles. The percentage of calcein release caused by the peptides was calculated by the equation.

$$\text{Leakage}\% = (F - F_0)/(F_t - F_0) \times 100 \quad (1)$$

where F is the fluorescence intensity achieved by the peptides, F_0 and F_t are intensities observed without and after Triton X-100 treatment, respectively.

Outer and Inner Membrane Permeabilities. Determination of the outer membrane permeability was performed by measuring the fluorescence intensity of NPN as described by Wu and Hancock.[14] Single colonies of *E. coli* grown on trypticase soy agar plates were inoculated in TSB (5 mL) and grown overnight at 37 °C. The suspension was diluted with TSB to an absorbance of 0.3–0.4 at 600 nm. A hundred microliters of 320 μM peptide solution were added to a mixture of the bacterial suspension (880 μL) and 250 μM NPN in acetone (20 μL). The outer membrane permeability was monitored by measuring the intensity at 420 nm (excited at 350 nm) for 10 min at 25 °C. An equivalent volume of water was used instead of peptide solution in control assay. Determination of the inner membrane permeability was performed by measuring galactosidase activity using ONPG as a substrate according to the procedure by Pellegrini et al.[15] A suspension of *E. coli* (10^4 cells mL^{-1}, 880 μL) was added to a solution of 250 μM ONPG in TSB medium (pH 7.4, 20 μL). After 15 min of incubation, 320 μM peptide solution (100 μL) was added. The inner membrane permeability was monitored by measuring the rate of *o*-nitrophenol production at 420 nm every 1 min. An equiv-

alent volume of water was used instead of the peptide solution in the control assay. Gramicidin S was used as positive control in both experiments.

Single Channel Measurements. Single channel experiments were carried out with pipette dipping patch clamp technique at room temperature.[22] The patch clamp pipettes were prepared from hematocrit hard glass capillaries. Settings in the pipette puller were adjusted to obtain a tip diameter of 1 μm. The pipettes were filled with solution of 0.5 M KCl buffered with 5 mM HEPES (pH 7.4) containing 100 nM peptides and a Ag–AgCl electrode was inserted in the pipette. Voltage was referenced to another Ag–AgCl electrode placed in the opposite side of the bilayer. The pipette tip was immersed in a Petri-dish filled with the same buffer without peptides. After immersion of the pipette, DPhPC phospholipid monolayer was spread on the surface of the dish solution by carefully adding to the edge of the dish 0.5–1.0 μL of a 10 mg mL^{-1} solution of the lipid dissolved in hexane. Before any movement of the electrode, 10 min were allowed for the evaporation of the solvent from the surface of the solution. Amplified single-channel currents were filtered at 1 or 2 kHz and analyzed using Axograph 3.5 (Axon Instruments, Inc.). The following cylindrical-bundle model was used to estimate the pore sizes of the helix bundle and number of helices involved in the bundle.[18]

$$G = \pi r^2/\rho(l + \pi r/2) \quad (2a)$$

$$r = R[1/\sin(\pi/N) - 1] \quad (2b)$$

where G is observed conductance value, R is radius of helix, l is helix length, r is radius of pore, ρ is resistivity of solution,[23] and N is number of aggregated helices respectively.

We wish to thank Prof. N. Fujii of Kinki University and Prof. Y. Shimohigashi of Kyushu University for carrying out the MALDI-TOFMS. We thank Mr. M. Nakahara, Ms. K. Hashimoto, and Dr. H. Yamaguchi for carrying out the initial experiments.

References

1 a) H. Duclohier, G. Molle, G. Spach, *Biophys. J.* **1989**, *56*, 1017. b) S. Oiki, W. Danho, M. Montal, *Proc. Natl. Acad. Sci. U.S.A.* **1988**, *85*, 2393.

2 a) Y. Shai, *Pept. Science* **2002**, *66*, 236. b) C. L. Bevins, M. Zasloff, *Annu. Rev. Biochem.* **1990**, *59*, 395. c) R. E. W. Hancock, G. Diamond, *Trends Microbiol.* **2000**, *8*, 402.

3 a) K. Anzai, M. Hamasuna, H. Kadono, S. Lee, H. Aoyagi, Y. Kirino, *Biochim. Biophys. Acta* **1991**, *1064*, 256. b) T. Iwata, S. Lee, O. Oishi, H. Aoyagi, M. Ohno, K. Anzai, Y. Kirino, G. Sugihara, *J. Biol. Chem.* **1994**, *269*, 4928.

4 a) B. L. Kagan, M. E. Selsted, T. Ganz, R. I. Lehrer, *Proc. Natl. Acad. Sci. U.S.A.* **1990**, *87*, 210. b) S. J. Ludtke, K. He, W. T. Heller, T. A. Harroun, L. Yang, H. W. Huang, *Biochemistry* **1996**, *35*, 13723.

5 Y. Agawa, S. Lee, S. Ono, H. Aoyagi, M. Ohno, T. Taniguchi, K. Anzai, Y. Kirino, *J. Biol. Chem.* **1991**, *266*, 20218.

6 N. Ohmori, T. Niidome, T. Hatakeyama, H. Mihara, H. Aoyagi, *J. Pept. Res.* **1998**, *51*, 103.

7 T. Niidome, N. Matsuyama, M. Kunihara, T. Hatakeyama, H. Aoyagi, *Bull. Chem. Soc. Jpn.* **2005**, *78*, 473.

8 a) M. Dathe, M. Schümann, T. Wieprecht, A. Winkler, M. Beyermann, E. Krause, K. Matsuzaki, O. Murase, M. Bienert, *Biochemistry* **1996**, *35*, 12612. b) M. Dathe, T. Wieprecht, H. Nikolenko, L. Handel, W. L. Maloy, D. L. MacDonald, M. Beyermann, M. Bienert, *FEBS Lett.* **1997**, *403*, 208.

9 D. Eisenberg, *Annu. Rev. Biochem.* **1984**, *53*, 595.

10 a) G. Saberwal, R. Nagaraj, *Biochim. Biophys. Acta* **1994**, *1197*, 109. b) T. Wieprecht, M. Dathe, R. M. Epand, M. Beyermann, E. Krause, W. L. Maloy, D. L. MacDonald, M. Bienert, *Biochemistry* **1997**, *36*, 12869.

11 a) J. H. Davis, D. M. Clare, R. S. Hodges, M. Bloom, *Biochemistry* **1983**, *22*, 5298. b) J. C. Huschilt, B. M. Millman, J. H. Davis, *Biochim. Biophys. Acta* **1989**, *979*, 139.

12 H. Mihara, T. Kanmera, M. Yoshida, S. Lee, H. Aoyagi, T. Kato, N. Izumiya, *Bull. Chem. Soc. Jpn.* **1987**, *60*, 697.

13 H. G. Labischinski, G. Barnickel, H. Bradaczek, D. Naumann, E. T. Rietschel, P. Giesbrecht, *J. Bacteriol.* **1985**, *162*, 9.

14 M. Wu, R. E. W. Hancock, *J. Biol. Chem.* **1999**, *274*, 29.

15 A. Pellegrini, C. Dettling, U. Thomas, P. Hunziker, *Biochim. Biophys. Acta* **2001**, *1526*, 131.

16 S. Kobayashi, K. Takeshima, C. B. Park, S. C. Kim, K. Matsuzaki, *Biochemistry* **2000**, *39*, 8648.

17 G. Baumann, P. Mueller, *J. Supramol. Struct.* **1974**, *2*, 538.

18 M. S. P. Sansom, *Eur. Biophys. J.* **1993**, *22*, 105.

19 J. M. Scholtz, H. Qian, E. J. York, J. M. Stewart, R. L. Baldwin, *Biopolymers* **1991**, *31*, 1463.

20 K. Yoshida, Y. Mukai, T. Niidome, C. Takashi, Y. Tokunaga, T. Hatakeyama, *J. Pept. Res.* **2001**, *57*, 119.

21 S. Lee, H. Mihara, H. Aoyagi, T. Kato, N. Izumiya, N. Yamasaki, *Biochim. Biophys. Acta* **1986**, *862*, 211.

22 B. A. Suarez-Isla, K. Wan, J. Lindstrom, M. Montal, *Biochemistry* **1983**, *22*, 2319.

23 R. A. Robinson, R. H. Stokes, *Electrolyte Solutions*, 2nd ed., Butterworths, London, **1970**.